CHAPTER 187

WAVE BREAKING AND INDUCED NEARSHORE CIRCULATIONS

Ole R. Sørensen †, Hemming A. Schäffer†, Per A. Madsen†, and Rolf Deigaard‡

ABSTRACT

Wave breaking and wave induced currents are studied in two horizontal dimensions. The wave-current motion is modelled using a set of Boussinesq type equations including the effects of wave breaking and runup. This is done without the traditional splitting of the phenomenon into a wave problem and a current problem. Wave breaking is included using the surface roller concept and runup is simulated by use of a modified slot-technique. In the environment of a plane sloping beach two different situations are studied. One is the case of a rip channel and the other concerns a detached breakwater parallel to the shoreline. In both situations wave driven currents are generated and circulation cells appear. This and many other nearshore physical phenomena are described qualitatively correct in the simulations.

1. INTRODUCTION

State of the art models for wave driven currents are based on a splitting of the phenomenon into a linear wave problem, described e.g. by the mild-slope equation, and a current problem, described by depth-integrated flow equations including radiation stress. Wave-current interaction effects such as current refraction and wave blocking may be included in these systems by successive and iterative model executions.

A more direct approach to the problem would be the use of a time domain Boussinesq model which automatically includes the combined effects of wave-wave and wave-current interaction in shallow water without the need for explicit formulations of the radiation stress. In the present work this direct approach is used in the study of wave-induced current phenomena in two horizontal dimensions.

The drawback of traditional Boussinesq models is that they cannot reproduce the effects of wave breaking. This precludes the modelling of surf conditions and thus the primary cause of wave driven currents. Prüser (1991) and Kabiling and Sato (1993) have modelled the effects of wave breaking by

† International Research Center for Computational Hydrodynamics (ICCH), Danish Hydraulic Institute, Agern Allé 5, DK-2970 Hørsholm, Denmark

‡ Institute of Hydrodynamics and Hydraulic Engineering (ISVA), Technical University of Denmark, DK-2800 Lyngby, Denmark

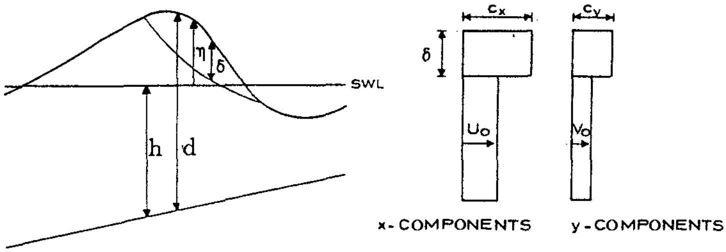

Figure 1 Cross-section and components of assumed velocity profile of a breaking wave with a surface roller.

including eddy viscosity terms in the equations. In general this approach tends to smear out the effects of breaking over the whole wave cycle. Thus basic physical phenomena like, for example, the pronounced vertical asymetry in breaking waves may not be reproduced.

Schäffer et al. (1992, 1993) incorporated wave breaking in a Boussinesq model by assuming a redistribution of momentum as a surface roller develops, taking the roller to be a passive bulk of water moving with the wave celerity. Accordingly, the vertical distribution of the horizontal velocity was approximated by the simple profile shown in Fig. 1. This was originally suggested by Svendsen (1984). Based on the idea of Deigaard (1989) the surface rollers were identified by a simple geometrical method. Despite the rather simple approach the results for e.g. wave height decay and set-up were promising. This work continues in two directions. One is confined to cross-shore processes (Madsen et al., 1994) while the other (present paper) deals with obliquely incident waves and wave induced circulations.

A number of coastal wave phenomena, such as the generation of infragravity waves, are sensitive to the conditions at the shoreline. For example, a natural beach tends to reflect most energy at low frequencies, while energy in the high frequency range is almost fully dissipated. Reproducing this as well as many other physical phenomena in a numerical model requires a runup condition allowing for a moving boundary. In the present model the formulation of such a shoreline boundary condition is based on a modified version of the slot-technique described by Tao (1983). This method is described in Madsen et al. (1994).

2. WAVE BREAKING AND RUNUP IN A BOUSSINESQ MODEL

2.1. Governing equations

Assuming the simplified velocity profile shown in Fig. 1 to be valid in case of wave breaking, the following modified version of the Boussinesq equations appear

$$\frac{\partial p}{\partial t} + \frac{\partial}{\partial x}\left(\frac{p^2}{d}\right) + \frac{\partial}{\partial y}\left(\frac{pq}{d}\right) + \frac{\partial R_{xx}}{\partial x} + \frac{\partial R_{xy}}{\partial y} + gd\frac{\partial \eta}{\partial x} + \psi_1 + \frac{\tau_x}{\rho} = 0 \quad (1a)$$

$$\frac{\partial q}{\partial t} + \frac{\partial}{\partial y}\left(\frac{q^2}{d}\right) + \frac{\partial}{\partial x}\left(\frac{pq}{d}\right) + \frac{\partial R_{yy}}{\partial y} + \frac{\partial R_{xy}}{\partial x} + gd\frac{\partial \eta}{\partial y} + \psi_2 + \frac{\tau_y}{\rho} = 0 \tag{1b}$$

Here (p, q) is the depth integrated velocity in the Cartesian coordinate system (x,y), $d = h + \eta$ is the instantaneous depth and η is the surface elevation. The definition of the surface roller terms are

$$R_{xx} \equiv \delta \frac{\left(c_x - \frac{p}{d}\right)^2}{1 - \frac{\delta}{d}} \tag{2a}$$

$$R_{xy} \equiv \delta \frac{\left(c_x - \frac{p}{d}\right)\left(c_y - \frac{q}{d}\right)}{1 - \frac{\delta}{d}} \tag{2b}$$

$$R_{yy} \equiv \delta \frac{\left(c_y - \frac{q}{d}\right)^2}{1 - \frac{\delta}{d}} \tag{2c}$$

as derived by Schäffer et al. (1992, 1993). Here $\delta = \delta(x, y, t)$ is the thickness of the surface roller determined in a heuristic geometrical way as given below. Components of the wave celerity are denoted c_x and c_y.

The terms denoted ψ are dispersive Boussinesq type terms which in shallow water may be taken from Peregrine (1967). Here we use the version derived by Madsen et al. (1991) and Madsen and Sørensen (1992):

$$\begin{aligned}\psi_1 \equiv & -(B + \frac{1}{3})h^2\left(\frac{\partial^3 p}{\partial x^2 \partial t} + \frac{\partial^3 q}{\partial x \partial y \partial t}\right) - Bgh^3\left(\frac{\partial^3 \eta}{\partial x^3} + \frac{\partial^3 \eta}{\partial x \partial y^2}\right) \\ & - h\frac{\partial h}{\partial x}\left(\frac{1}{3}\frac{\partial^2 p}{\partial x \partial t} + \frac{1}{6}\frac{\partial^2 q}{\partial y \partial t} + 2Bgh\frac{\partial^2 \eta}{\partial x^2} + Bgh\frac{\partial^2 \eta}{\partial y^2}\right) \\ & - h\frac{\partial h}{\partial y}\left(\frac{1}{6}\frac{\partial^2 q}{\partial x \partial t} + Bgh\frac{\partial^2 \eta}{\partial x \partial y}\right)\end{aligned} \tag{3a}$$

$$\begin{aligned}\psi_2 \equiv & -(B + \frac{1}{3})h^2\left(\frac{\partial^3 q}{\partial y^2 \partial t} + \frac{\partial^3 p}{\partial x \partial y \partial t}\right) - Bgh^3\left(\frac{\partial^3 \eta}{\partial y^3} + \frac{\partial^3 \eta}{\partial x^2 \partial y}\right) \\ & - h\frac{\partial h}{\partial y}\left(\frac{1}{3}\frac{\partial^2 q}{\partial y \partial t} + \frac{1}{6}\frac{\partial^2 p}{\partial x \partial t} + Bgh\frac{\partial^2 \eta}{\partial x^2} + 2Bgh\frac{\partial^2 \eta}{\partial y^2}\right) \\ & - h\frac{\partial h}{\partial x}\left(\frac{1}{6}\frac{\partial^2 p}{\partial y \partial t} + Bgh\frac{\partial^2 \eta}{\partial x \partial y}\right)\end{aligned} \tag{3b}$$

as valid for a wider range of water depths using $B = 1/15$.

Bottom friction is modelled using

$$(\tau_x, \tau_y) \equiv \rho \frac{\sqrt{p^2 + q^2}}{C^2 d^2}(p, q) \tag{4}$$

where $C = Md^{1/6}$ is the Chezy resistance $(m^{1/2}/s)$, M being the Manning number. This formulation is very simplified and does not represent the effect of turbulent interaction between oscillatory boundary layers and the mean flow.

The equation for conservation of mass is unchanged

$$\frac{\partial \eta}{\partial t} + \frac{\partial p}{\partial x} + \frac{\partial q}{\partial y} = 0 \tag{5}$$

2.2. Determination of the surface roller

The determination of the surface roller $\delta(x, y, t)$ (see Fig. 1) is made as described in detail by Schäffer et al. (1992) and summarized below, beginning with the case of only one horizontal dimension.

Breaking sets in when and where the local slope exceeds a certain value $\tan \phi_B$ and the actual point is taken as the instantaneous toe of a surface roller. At the given instant, the roller is then taken to be constituted by the water above the tangent of angle ϕ_B starting at the roller toe and going in the direction opposite of wave propagation. After incipient breaking the procedure is the same except now decreasing angles $\phi = \phi(t)$ are used in place of ϕ_B. The system keeps track on the age of each surface roller and applies a value given by

$$\tan \phi(t) = \tan \phi_0 + (\tan \phi_B - \tan \phi_0) \exp\left[-\ln 2 \frac{t - t_B}{t_{1/2}}\right] \tag{6}$$

Here ϕ_0 is the terminal value of $\phi(t)$, t_B is the time of incipient breaking and $t_{1/2}$ is the half time for $\tan \phi(t)$. The following values were used in all the results presented below: $\phi_B = 20°$, $\phi_0 = 10°$ and $t_{1/2} = T/10$ where T is a typical period of the waves. After the determination of the surface roller in each time step, δ is multiplied by a shape factor f_δ prior to the inclusion in the governing equations. A value of $f_\delta = 2$ was used.

In two horizontal dimensions the toe of the roller becomes a curve instead of a single point and the tangent becomes a set of generating lines determined by the instantaneous local angle $\phi(t)$. Whereas $\phi(t)$ in the one-dimensional case is constant within each roller, it is allowed to have a lateral variation in the two-dimensional case. This lateral variation of $\phi(t)$ within each surface roller must be allowed since, for example, when oblique regular waves break on an alongshore uniform beach both the initial and the final stage of the breaking processs will be represented within the same roller. The lateral variation of $\phi(t)$ is allowed for by keeping track on the surface roller age along the orthogonal to the roller toe curve. Thus, between each pair of generating line used for the roller determination, $\phi(t)$ decays according to (6).

2.3. Solution technique

The differential equations are discretized using a time-centered implicit scheme with variables defined on a space-staggered rectangular grid. The method is based on the Alternating Direction Implicit algorithm. For more details of the solution procedure reference is made to Abbott et al. (1978, 1981, 1984), McCowan (1978, 1984) and Madsen et al. (1991, 1992).

The finite-difference approximation of the spatial derivatives is generally a straight-forward mid-centering. However, in the present work we have treated the nonlinear convective terms somewhat differently. The use of high-order central schemes for the discretization of convective terms is known to introduce non-physical oscillations in regions with large gradients of the convected variable. Typically these appear around corners of structures e.g. at the tip of

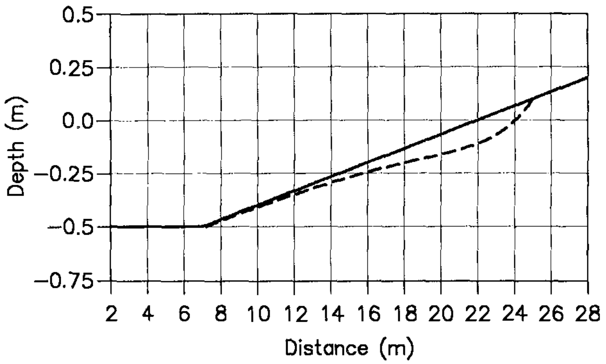

Figure 2 Beach profiles for the rip channel test. (——): along a plane beach section and (- - -): along the rip channel.

a breakwater, in regions of strong wave-induced circulations, and in the bore-like stage in the inner surf zone. The classical first-order upwinding scheme is non-oscillatory, but introduces an unacceptable artificial diffusion. Higher-order upwinding schemes significantly reduce this diffusion, but still overshoots and undershoots may occur in the solution.

A number of oscillation-free schemes have been proposed in the literature, especially within the field of compressible flows with strong shocks. A disadvantage of these schemes is that they increase the computational cost significantly. For this reason a more simple approach has been used here: a first-order upwinding scheme is applied in sharply varying regions, that is in regions where the depth-integrated velocity is non-monotonic, and elsewhere second-order (quadratic) upwinding is applied.

3. NUMERICAL SIMULATIONS

In principle, the model can be used for a wide range of coastal phenomena. However, since the inclusion of wave breaking is more or less based on the spilling-breaker assumption, it is primarily suited for mild slopes and rather steep waves.

We have chosen two different situations with waves normally incident on a plane sloping beach but with some alongshore non-uniformity to trigger nearshore circulation. In the first example a rip channel is present while the other concerns a detached breakwater parallel to the shoreline. In both examples the bathymetry has a crosshore line af symmetry. In case of normally incident unidirectional waves the numerical computation was only made in half of the region in question. This reduced the computational cost, but precluded possible instabilities of currents along the line of symmetry.

3.1. A plane beach with a rip channel

The first example is chosen according to laboratory experiments reported by Hamm (1992). The wave basin was 30m by 30m and the bathymetry was a a plane sloping beach of 1:30 with a rip channel excavated along the centerline. The profiles of the rip channel and the plane beach is shown in Fig. 2. Two of

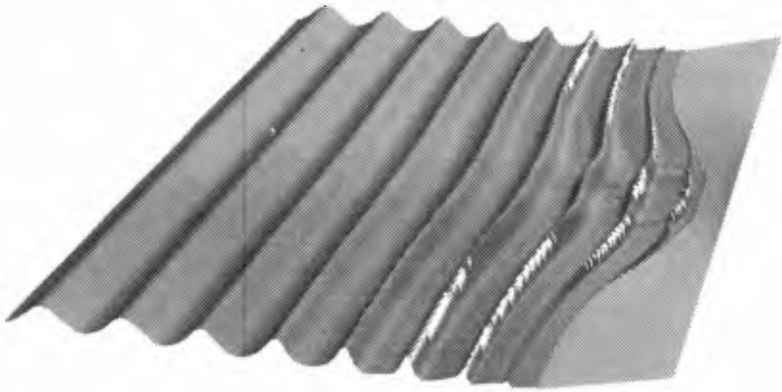

Figure 3 Birds view of the free surface elevation for the rip channel case with regular waves. The surface rollers are shown in white.

Hamm's test cases were modelled numerically. In the first test the waves were regular with a period of 1.25s and a wave height of 0.07m and unidirectional with normal incidence. In the second test the incident waves were multidirectional and irregular and sampled from a JONSWAP spectrum with a peak period of 1.25s and a significant wave height of 0.07m and with a directional spreading corresponding to a $\cos^6\theta$-distribution. In both cases a Manning number of $72\text{m}^{1/3}/\text{s}$ was used in the bed friction term. The grid spacing was 0.05m and the time step 0.01s.

For the regular-wave case a birds view of the surface elevation (in a subdomain) is shown in Fig. 3. The surface rollers are shown in white. Due to the increased depth and due to depth refraction by the rip channel incipient breaking occurs comparatively close to shore along the centerline. Here the setup is quite small and the larger setup appearing away from the rip channel gives an alongshore gradient in the mean water surface forcing a current towards the centerline. Here the flows from the two sides join to form a rip current and two symmetrical circulation cells appear.

The effect of the rip current on the wave height counteracts the effect of depth refraction and hence incipient breaking starts locally at the centerline. The rip current also causes a small local oscillation in the wave crest occuring at the same place. These phenomena also show up in a video of the experiment kindly supplied by Hamm.

A vector plot of the depth-integrated velocity averaged over one wave period is shown in Fig. 4. A subdomain is shown in order to focus one of the circulation cells which has developed. A pronounced rip current is seen along the centerline of the bathymetry i.e. at the top of the figure.

Figure 5 shows the cross-shore variation of the rip current computed as the time-average of the velocity below the roller, U_0. For reasons of symmetry the rip current was bound to be directed exactly perpendicular to the shore. In Hamm's experiments the measured rip current showed a significant deviation from this direction. It is unclear whether this was due to imperfections in the supposedly symmetrical experiment or if instabilities of the rip current could

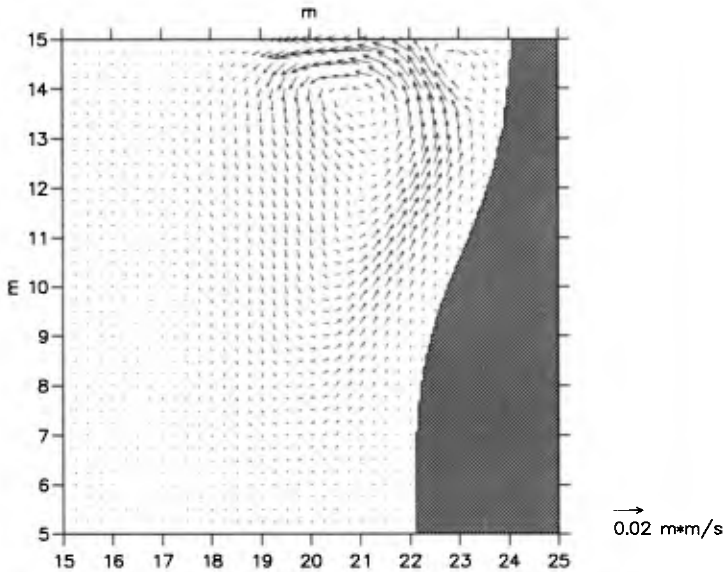

Figure 4 Depth-integrated velocity for the situation shown in Fig. 3 focusing on a circulation cell.

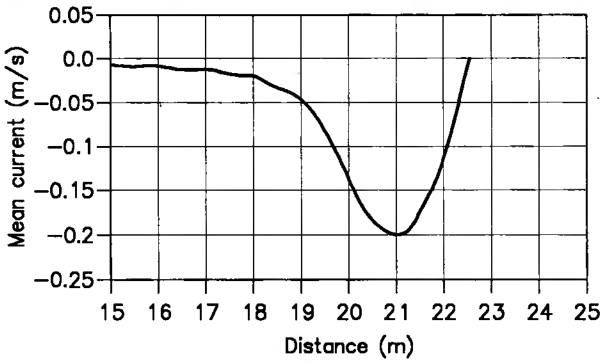

Figure 5 Rip current along the rip channel for the regular-wave case.

be responsible. With regard to the order of magnitude of the rip current speed, agreement was found between the numerical simulation and the experimental results.

Figure 6a shows the wave height at some distance from the rip channel where the beach is a plane slope. A similar plot but along the excavated beach at the centerline is shown in Fig. 6b. The measurements of Hamm are included for comparison and the agreement is quite good. The large variation of the rip

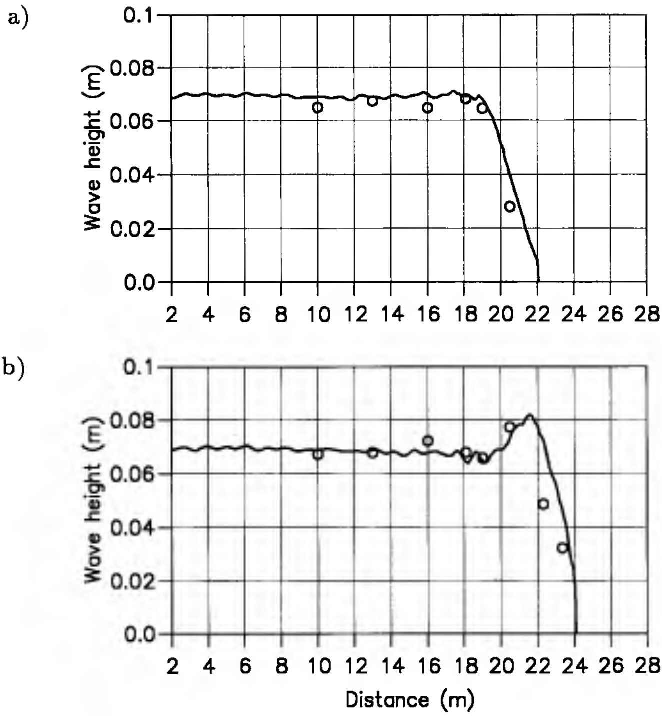

Figure 6 Comparison of the cross-shore wave height variation for the regular wave case of the rip channel case a) along a plane beach section and b) along the rip channel. (—): numerical simulation, (o): measurements by Hamm (1992).

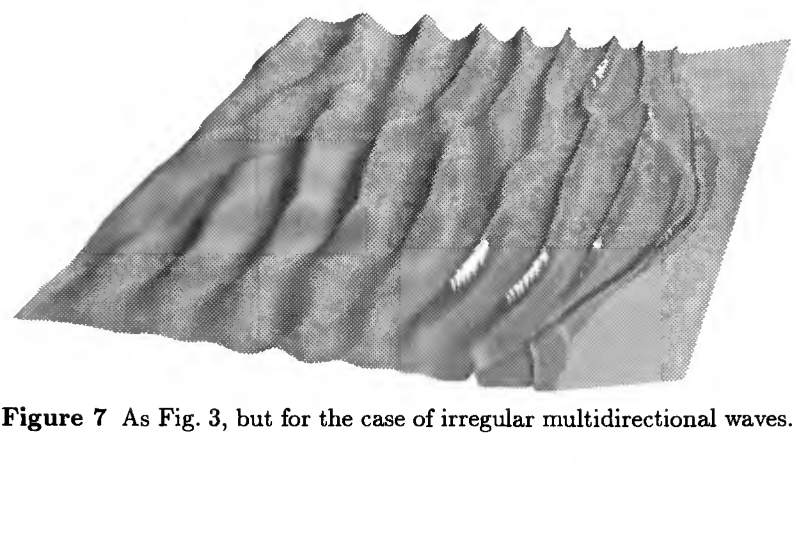

Figure 7 As Fig. 3, but for the case of irregular multidirectional waves.

current (see Fig. 5) is seen to cause a pronounced increase in the wave height in Fig. 6b.

Figure 7 shows a birds view of the surface elevation for the multidirectional irregular-wave case. The duration of this simulation was too short to give confidential statistics precluding comparison of significant wave height and average velocities with the experimental values.

3.2. A plane beach with a detached breakwater

The second example concerns a plane sloping beach of 1:50 with a 300m long detached breakwater placed at a still water depth of 6m i.e. 300m from the shore. Regular, unidirectional waves of normal incidence, a period of 8s and a wave height of 2m were generated at a depth of 10m. The computational domain extended 700m offshore and 600m alongshore from the line of symmetry and the seaward side of the breakwater was treated as land. The grid spacing was 1m and the time step was 0.08s. Bed friction was modelled using a Manning number of $32m^{1/3}/s$.

A birds view of the elevation is shown in Fig. 8. Again, surface rollers are shown in white. The diffraction around the breakwater gives the expected oscillations in the wave height along the wave crests, see Fig. 9 for the wave height variation. This further results in scattered incipient breaking, but the surface rollers quickly merge extending the breaking process to cover the long crested wave. In the simulation the roller dissapears before the waves reach the shore. This is an unwanted side effect of a spatial smoothing which for reasons of stability was applied in the vicinity of the swash zone. Note the nonlinear cross-wave pattern close to the shore in lee of the breakwater.

The depth-integrated velocity averaged over one wave period is shown in Fig. 10. The maximum current speed behind the breakwater is approximately 0.7m/s and it occurs about 80m from the shoreline near the edge of the breakwater. In addition to the expected circulation cell, a local phenomenon resembling thin rip currents appears further away from the breakwater. This is more pronounced in Fig. 11 showing the time-average of the velocity below the roller, (U_0, V_0). This velocity field includes the depth averaged undertow. The thin rip currents may be caused by the lateral variation of the wave height as created by the diffraction around the breakwater. However, this remains to be studied further.

ACKNOWLEDGEMENT

This work has been financed mainly by the Danish National Research Foundation and partly by the Commission of the European Communities, Directorate General for Science, Research, and Development under MAST contract No. MAS2-CT92-0027.

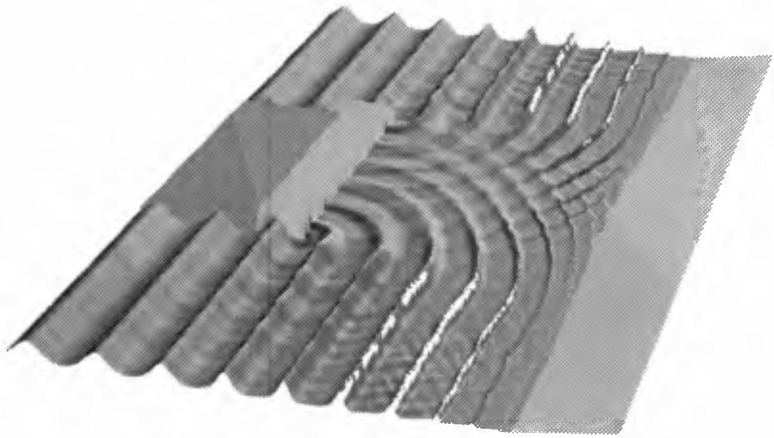

Figure 8 Birds view of the free surface elevation for the detached breakwater case with regular waves. The surface rollers are shown in white.

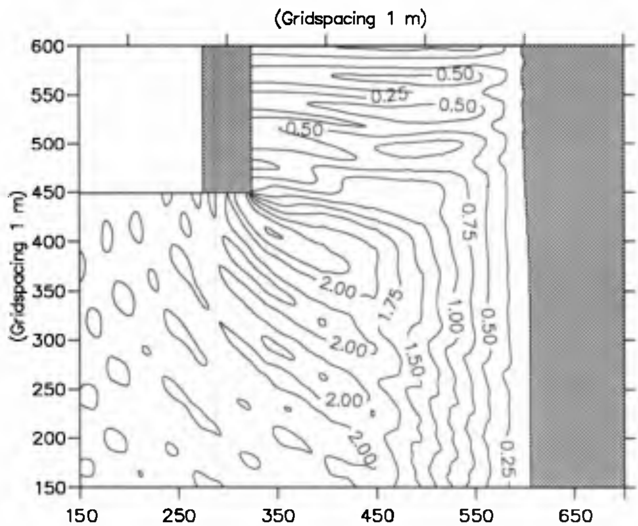

Figure 9 Wave height variation for the situation in Fig. 8, showing only half of the region.

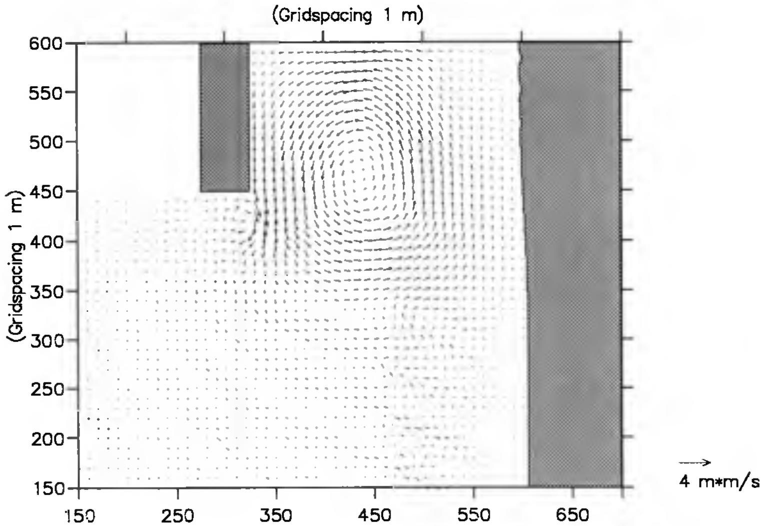

Figure 10 Time-averaged and depth-integrated velocity corresponding to Fig. 9.

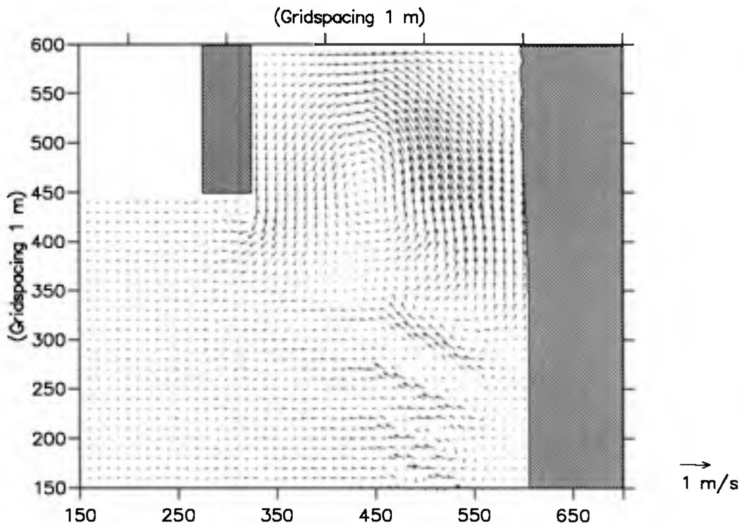

Figure 11 Time-average of the velocity beneath the surface rollers corresponding to Fig. 10.

REFERENCES

Abbott, M. B., H. M. Petersen and O. Skovgaard (1978). On the numerical modelling of short waves in shallow water. *J. Hydraul. Res*, **16**(3), 173-203.

Abbott, M. B., A. D. McCowan and I. R. Warren (1981). Numerical modelling of free-surface flows that are two-dimensional in plan. In: *Transport Models for Inland and Coastal Water*, Symp. Predictive Ability, Academic Press, New York, N.Y.

Abbott, M. B., A. D. McCowan and I. R. Warren (1984). Accuracy of short wave numerical models, J. Hydraul. Engrg. **110**(10), 1287-1301.

Deigaard, R. (1989). Mathematical modelling of waves in the surf zone. Prog. Rep. 69, ISVA, Technical University of Denmark, Lyngby, 47-59.

Hamm, L. (1992). Directional nearshore wave propagation over a rip channel: and experiment. Proc. 23rd Int. Conf. Coastal Eng., Venice Italy, 1992, ASCE, New York, 1993.

Kabiling, M. B. and S. Sato (1993). Two-dimensional nonlinear dispersive wave-current and three-dimensional beach deformation model. *Coastal Engrg. in Japan* **36**, 196-212.

Madsen, P. A., R. Murray and O. R. Sørensen (1991). A new form of the Boussinesq equations with improved linear dispersion characteristics. Part 1. *Coastal Engrg.* **15**, 371-388.

Madsen, P. A. and O. R. Sørensen (1992). A new form of the Boussinesq equations with improved linear dispersion characteristics. Part 2. A slowly-varying bathymetry. *Coastal Engrg.* **18**, 183-204.

Madsen, P.A., O.R. Sørensen, and H.A. Schäffer (1994). Time domain modelling of wave breaking, runup, and surf beats. This conference.

McCowan, A. S. (1978). Numerical simulation of shallow water waves. Proc. 4th Austr. Conf. Coastal and Ocean Eng., Adelaide, Australia.

McCowan, A. S. (1984). Developments in numerical short wave modelling. Proc. 5th Austr. Conf. Coastal and Ocean Eng., Perth, Australia.

Peregrine, D. H. (1967). Long waves on a beach. *J. Fluid Mech.* **27**(4), 815-827.

Prüser, H.-H. (1991). Zur Interaktion von Wellen und Strömung im flachen Wasser. *Report No. 30*, Institut für Strömungsmechanik und elektronisches Rechnen im Bauwesen, Universität Hannover.

Schäffer, H.A., R. Deigaard, and P.A. Madsen (1992). A two-dimensional surf zone model based on the Boussinesq equations. Proc. 23rd Int. Conf. Coastal Eng., Venice Italy, 1992, ASCE, New York, 1993.

Schäffer, H.A., P.A. Madsen, and R. Deigaard (1993). A Boussinesq model for waves breaking in shallow water. Coastal Engineering, Vol. 20, 185-202.

Svendsen, I. A. (1984). Wave heights and setup in a surf zone. *Coastal Engrg.*, **8**(4), 303-329.

Tao, J. (1983). Computation of wave run-up and wave breaking. Internal Report, 40 pp, Danish Hydraulic Institute.